P2X4 Forms Functional ATP-activated Cation Channels on Lysosomal Membranes Regulated by Luminal pH*

Peng Huang[‡1], Yuanjie Zou[‡1], Xi Zoë Zhong[‡1], Qi Cao[‡], Kexin Zhao[‡], Michael X. Zhu[§], Ruth Murrell-Lagnado[¶], and Xian-Ping Dong[‡2]

From the [‡]Department of Physiology and Biophysics, Dalhousie University, Sir Charles Tupper Medical Building, 5850 College Street, Halifax, Nova Scotia B3H 4R2, Canada, the [§]Department of Integrative Biology and Pharmacology, The University of Texas Health Science Center at Houston, Houston, Texas 77030, and the [¶]Department of Pharmacology, University of Cambridge, Tennis Court Road, Cambridge CB2 1PD, United Kingdom

Background: Ca^{2+}-permeable P2X4 channels are expressed in lysosomes.
Results: Lysosomal P2X4 channels are activated by ATP from the luminal side in a pH-dependent manner.
Conclusion: P2X4 forms functional ATP-activated cation channels on lysosomal membranes regulated by luminal pH.
Significance: Expanding the research of lysosomal Ca^{2+} signaling by adding another Ca^{2+} permeable channel on the lysosomal membranes.

P2X receptors are commonly known as plasma membrane cation channels involved in a wide variety of cell functions. The properties of these channels have been extensively studied on the plasma membrane. However, studies in amoeba suggest that P2X receptors are also present intracellularly and involved in vesicle fusion with the plasma membrane. Recently, it was shown that in addition to plasma membrane expression, mammalian P2X4 was also localized intracellularly in lysosomes. However, it was not clear whether the lysosomal P2X4 receptors function as channels and how they are activated and regulated. In this paper, we show that both P2X4 and its natural ligand, ATP, are enriched in lysosomes of COS1 and HEK293 cells. By directly recording membrane currents from enlarged lysosomal vacuoles, we demonstrated that lysosomal P2X4 formed channels activated by ATP from the luminal side in a pH-dependent manner. While the acidic pH at the luminal side inhibited P2X4 activity, increasing the luminal pH in the presence of ATP caused P2X4 activation. We further showed that, as for the plasma membrane P2X4, the lysosomal P2X4 was potentiated by ivermectin but insensitive to suramin and PPADS, and it permeated the large cation *N*-methyl-D-glucamine upon activation. Our data suggest that P2X4 forms functional ATP-activated cation channels on lysosomal membranes regulated by luminal pH. Together with the reported fusion effect of intracellular P2X in lower organisms, we speculate that the lysosome-localized P2X4 may play specific roles in membrane trafficking of acidic organelles in mammalian cells.

Purinergic signaling is one of the most important signaling pathways involved in cell communication in mammals. It is mediated by a large family of receptors known as the purinergic receptors that respond to extracellular purines. Purinergic receptors are divided into two groups, *i.e.* ligand-gated ion channels (P2X receptors) and G-protein-coupled receptors (P2Y and adenosine receptors). P2X receptors are ligand-gated non-selective cation channels that open in response to the binding of ATP at the extracellular side (1, 2). To date, seven non-allelic genes have been identified to encode P2X subunits, P2X1 through P2X7 (1, 3).

P2X4 receptor is found in neurons as well as epithelia, endothelia, and immune cells. Activation of P2X4 on the plasma membrane (PM)[3] allows cations, such as Na^+ and Ca^{2+}, to enter the cell, leading to membrane depolarization and the activation of various Ca^{2+}-sensitive intracellular processes, including the regulation of cardiac function, ATP-mediated cell death, pain sensation, and immune response. Different from many other P2X receptors, P2X4 on the PM is specifically potentiated by ivermectin, a bacterium-derived broad spectrum antiparasitic agent (4). The P2X4 receptor is also relatively insensitive to the common P2 receptor antagonists, suramin and PPADS. Interestingly, activation of P2X4 leads to increased permeability to the large cation, *N*-methyl-D-glucamine ($NMDG^+$), indicating activation induced pore dilation (1, 3).

It has been shown that P2X4 receptors on the PM are internalized via clathrin- and dynamin-dependent endocytosis (5). Eventually, some P2X4 receptors are trafficked to lysosomal membranes (2). Although the physiological functions of P2X4 channels localized at the cell surface are well-established, how lysosomal P2X4 channels function remained unexplored. Therefore, it is interesting to know whether the lysosome-lo-

[3] The abbreviations used are: PM, plasma membrane; PPADS, pyridoxalphosphate-6-azophenyl-2′,4′-disulphonic acid; Lamp1, lysosomal-associated membrane protein 1; GPN, glycyl-phenylalanine 2-naphthylamide; PNS, postnuclear supernatant.

calized P2X4 receptors function as channels and how similar they are to their PM counterparts.

In this study, we directly measured P2X4 channel activity in intact lysosomes. We found that both ATP and P2X4 receptors were present in lysosomes, and the lysosomal P2X4 was activated by ATP at the luminal side in a pH-dependent manner. As for the channels on the PM, lysosomal P2X4 was potentiated by ivermectin but insensitive to suramin or PPADS. We also showed that as for their PM counterparts, the lysosomal P2X4 channels were permeable to the large cation $NMDG^+$. Our study characterized, for the first time, P2X4 channel function on the lysosomal membrane and elucidated the potential activation mechanism for lysosomal P2X4.

EXPERIMENTAL PROCEDURES

Cell Culture—COS1 and HEK293T cells were obtained from ATCC (Manassas, VA) and maintained in Dulbecco's Modified Eagle's Medium: Nutrient Mixture F-12 (DMEM/F12) supplemented with 10% fetal bovine serum (Invitrogen). Cells were cultured at 37 °C in a 5% CO_2 atmosphere. For some experiments, cells were seeded on 0.1% poly-lysine-coated coverslips and cultured for 24 h before further experiments. Cells from passage numbers 5–25 were used for subsequent assays.

Antibodies and Reagents—The following primary antibodies were used in immunofluorescent staining: anti-P2X4 (1:200, Alomone Labs, Jerusalem, Israel), anti-Lamp1 (1:250, H4A3, Developmental Studies Hybridoma Bank). Antibodies used for Western blotting were anti-Lamp1 (H4A3, 1:2,000); anti-Annexin V (1:2,000, Abcam); anti-GM130 (1:2,000, Abcam); anti-EEA1 (1:2,000, Abcam); anti-Complex II (1:2,000, Invitrogen); anti-GAPDH (1:5,000, Santa Cruz Biotechnology). HRP-conjugated goat anti-rabbit and goat anti-mouse antibodies were purchased from Santa Cruz Biotechnology and Bio-Rad and used at 1:1,000 and 1:10,000 dilutions, respectively. Alexa Fluor 594-conjugated goat anti-rabbit antibody, Alexa Fluor 488-conjugated goat anti-rat antibody, fluorescein-conjugated goat anti-mouse, and Texas Red-conjugated goat anti-mouse antibodies were from Invitrogen and were used at 1:250 dilution. LysoTracker DND-99 Red (Invitrogen, 50 nM) and Texas Red 10 kDa dextran (Invitrogen, 1 mg/ml) were used to label lysosomes. GPN (200 μM) was from Santa Cruz Biotechnology.

Immunocytochemistry—Cells grown on coverslips were washed with phosphate-buffered saline (PBS) twice and fixed in 4% paraformaldehyde in PBS for 15 min at room temperature. Fixed cells were permeabilized with 0.1% Triton X-100 in PBS for 5 min, then blocked with 3% bovine serum albumin in PBS for 60 min at room temperature. After three washes with PBS, cells were incubated with specific primary antibodies at 4 °C overnight. After three times washing with PBS, cells were incubated with Alexa Fluor 488-conjugated goat anti-mouse IgG, Alexa Fluor 594-conjugated goat anti-rabbit IgG, or fluorescein-conjugated goat anti-mouse IgG secondary antibodies for 45 min at room temperature in the dark. Images were acquired on a confocal laser microscope (LSM510, Zeiss) using a 63× oil-immersion objective lens.

Confocal Microscopy—Confocal fluorescent images were taken using an inverted Zeiss LSM510 confocal microscope with a 63× oil-immersion objective. Sequential excitation

wavelengths at 488 and 543 nm were provided by argon and helium-neon gas lasers, respectively. Emission filters BP500–550 and LP560 were used for collecting green and red images in channels one and two, respectively. After sequential excitation, green and red fluorescent images of the same cell were collected and analyzed using ZEN2009 software (Zeiss). The term colocalization refers to the coincident detection of above-background green and red fluorescent signals in the same region. The image size was set at 1,024 × 1,024 pixels.

Molecular Biology and Biochemistry—Rat P2X4 receptor with EGFP fused to the C terminus (rP2X4-GFP), and S341W-GFP were made as described previously (2). All constructs were confirmed by sequencing analysis and protein expression was verified by Western blotting. COS1 cells were transiently transfected using Lipofectamine 2000 (Invitrogen) with rP2X4-GFP and various P2X4 mutants for electrophysiology, biochemistry, live cell imaging, and confocal imaging.

Lysosome Isolation by Subcellular Fractionation—Lysosomes were isolated as described previously (6, 7). Briefly, cell lysates were obtained by Dounce homogenization in a homogenizing buffer (HM buffer; 0.25 M sucrose, 1 mM EDTA, 10 mM HEPES; pH 7.0), and then centrifuged at 1,500 × g (4200 rpm, Fisher, ST-16R, F15 rotor) at 4 °C for 10 min to remove the nuclei and intact cells. Postnuclear supernatants were then subjected to ultracentrifugation through a Percoll density gradient using a Beckman Optima L-90K ultracentrifuge. An ultracentrifuge tube was layered with 2.5 M sucrose, 18% Percoll in HM buffer and supernatant (top). The centrifugation was carried out at 90,000 × g (31,300 rpm), 4 °C, for 1 h using a Beckman Coulter 70.1 Ti rotor. Samples were fractionated into light, medium, and heavy membrane fractions. Heavy membrane fractions contained concentrated bands of cellular organelles and were further layered over a discontinuous iodixanol gradient, generated by mixing iodixanol in HM buffer with 2.5 M glucose (in v/v; 27, 22.5, 19, 16, 12, and 8%) and with osmolarity maintained at 300 mOsm for all solutions. After centrifugation at 4 °C for 2.5 h at 180,000 × g (44,200 rpm), each sample was divided into twelve fractions (0.5 ml each) for further analyses. Note that the biological and ionic compositions of the lysosomes were largely maintained due to the low rate of transport across the lysosomal membrane at 4 °C. Proteins were analyzed by standard Western blotting.

Measurement of ATP—Cells were incubated with quinacrine (5 μM) together with LysoTracker Red DND-99 (50 nM) for 30 min at 37 °C and chased for 1 h. Images were acquired using the confocal microscope (Zeiss) with the 63× oil-immersion objective by sequential excitation at 488 nm (emission at 505–525 nm) for quinacrine and 543 nm (emission at 560 nm) for Lyso-Tracker. The fluorescence images were collected and analyzed using ZEN2009 (Zeiss). A low laser power (< 0.5%) was used to avoid possible photo bleaching.

ATP contents in the buffer of freshly isolated lysosomes were measured in triplicates with the microplate luminometer (Fluoroskan Ascent FL Microplate Fluorometer and Luminometer, Thermo Scientific) using the Adenosine 5′-triphosphate Bioluminescent Assay kit (FLAA, Sigma) according to the manufacturer's instructions. In each measurement, a standard curve was established. Samples, either culture media or lysosomal fractions,
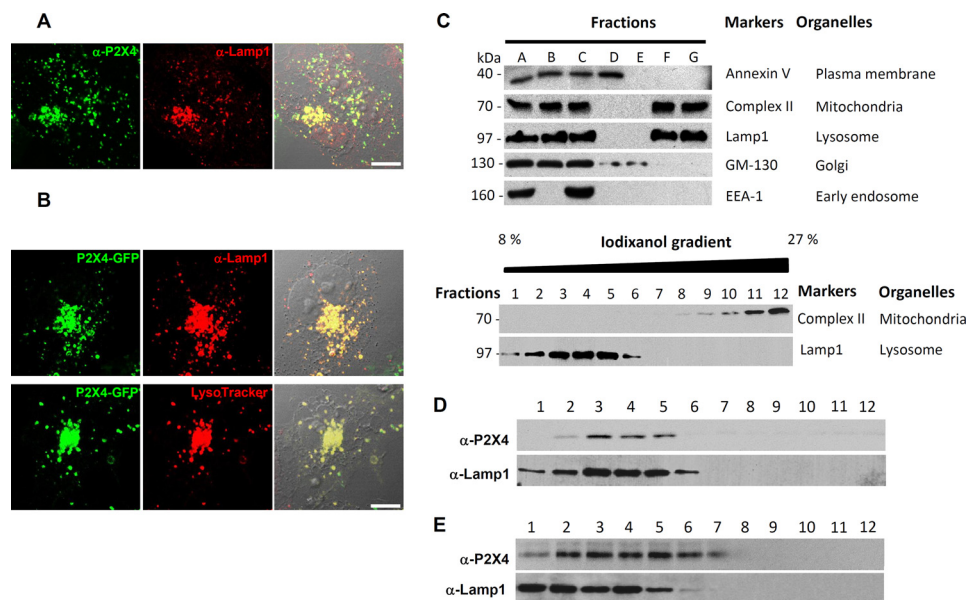
FIGURE 1. **Lysosomal localization of P2X4.** *A,* co-staining of endogenous P2X4 and Lamp1 in COS1 cells. Scale bars, 10 μm. *B,* co-localization of heterologously expressed rP2X4-GFP with Lamp1 (*upper images*) and LysoTracker (*lower images*) in COS1 cells. Scale bars, 10 μm. *C,* isolation of lysosomal fractions from COS1 cells using two-step density gradient centrifugations. Fractions (*A,* cells lysate; *B,* pellet; *C,* PNS from 1000 $\times$ *g* centrifugation; *D,* light membrane fraction from PNS; *E,* medium membrane fraction from PNS; *F,* light membrane fraction in PNS-heavy membrane fraction; *G,* heavy membrane fraction in PNS-heavy membrane fraction) from each major step were collected and blotted using markers for subcellular organelles as indicated to identify and confirm fractions that contained lysosomes (*upper panel*). Fraction G was applied to the iodixanol gradient for separation of lysosomes (*fractions 2–5*) from mitochondria (*fractions 8–12*) (*lower panel*). *D,* detection of endogenous P2X4 ($\sim$70 kDa) in lysosomal fractions (*bands 1–6*) of COS1 cells prepared by density gradient ultracentrifugation. *E,* presence of heterologously expressed rP2X4-GFP ($\sim$100 kDa) in lysosomal fractions (*bands 1–6*) of transfected COS1 cells prepared by density gradient ultracentrifugation. Lamp1 is shown as a control.

were handled gently, and pH was adjusted to $\sim$7.8 for the optimal assay condition of ATP detection. All samples were kept on ice before measurement. Briefly, 100 μl of the ATP assay mix solution was added to the assay tube and allowed to stand at room temperature for 3 min to hydrolyze residual background ATP. Then 100 μl sample was added rapidly, gently mixed, and the plate was read immediately in a luminometer. Blank medium or buffer was always included and read in parallel for background, which was subtracted from sample readings.

Estimation of Mean ATP Concentration in the Lysosome—Lysosomes were isolated from $\sim$3 $\times$ 10^7 cells and ATP concentration (C) of the lysosome suspension was determined using FLAA as described above. In the assay, a total volume (V) of 200 μl was reached by mixing 100 μl lysosome suspension with 100 μl assay buffer.

The equation C $\times$ V = C$_{lysosome}$ $\times$ V$_{total\ lysosome}$ was used to calculate the lysosomal ATP concentration. Given that lysosomes make up 1–10% of the whole cell volume (8), this equation can be converted to C $\times$ V = C$_{lysosome}$ $\times$ (1~10)% $\times$ V$_{total\ cell}$.

To measure the size of COS1 cells, cells were seeded on coverslips, and Z-stacks were taken to measure the diameter of the cell before cells became flat. Based on the z-stack images, the mean radius (R_{cell}) of COS1 cells was determined to be 11.25 μm. Therefore, V$_{single\ cell}$ = 4/3 $\times$ π $\times$ R$_{cell}$^{3}.

To exam the yield of lysosome isolation, 1.5 $\times$ 10^7 cells were used for lysosome isolation using gradient fractionation to obtain fraction G. The same number of cells was collected to generate whole cell lysate. Fraction G and whole cell lysate were brought to the same volume using SDS loading buffer. Equal volume of samples was then resolved by 10% SDS-PAGE for Western blot analyses using anti-Lamp1. The ratio of Lamp1

band intensity in fraction G (which contains all the lysosomes used for the rement of ATP concentration) over that in whole cell lysate (which contains total lysosomes in the cell) was analyzed by ImageJ gel analysis. This ratio, representing the yield of lysosome isolation, was determined to be 66.6% $\pm$ 1.9% (n = 3) (Fig. 4*B*), which is in agreement with the manufacturer's manual.

The number of cells used for lysosome isolation was defined as N$_{cell}$. V$_{total\ cell}$ = V$_{single\ cell}$ $\times$ N$_{cell}$. Therefore, the equation for calculating C$_{Lysosome}$ is: C $\times$ V = C$_{lysosome}$ $\times$ (1~10) % $\times$ V$_{single\ cell}$ $\times$ N$_{cell}$ $\times$ 66.6% = C$_{lysosome}$ $\times$ (1~10) % $\times$ 4/3 $\times$ π $\times$ R$_{cell}$^{3} $\times$ N$_{cell}$ $\times$ 66.6% (Fig. 4, *A* and *B*).

Lysosomal Electrophysiology—Lysosomal electrophysiology was performed in isolated enlarged lysosomes using a modified patch-clamp method as described previously (9). Briefly, cells were treated for >2 h with 1 μM vacuolin-1, a lipophilic polycyclic triazine that can selectively increase the size of endosomes and lysosomes (10). Large vacuoles were observed in most vacuolin-1-treated cells. Enlarged vacuoles were also seen in some untreated P2X4-expressing cells and no obvious difference in P2X4 channel properties was detected between enlarged vacuoles obtained with or without vacuolin-1 treatment. Whole-lysosome recordings were performed on manually isolated enlarged lysosomes (6). In brief, a patch pipette was pressed against a cell and quickly pulled away to slice the cell membrane. This allowed enlarged lysosomes to be released into the recording chamber and identified by monitoring EGFP fluorescence. After formation of a gigaseal between the patch pipette and an enlarged lysosome, capacitance transients were compensated. Voltage steps of several hundred millivolts with

millisecond duration(s) were then applied to break the patched membrane and establish the whole-lysosome configuration.

Unless otherwise stated, bath (cytoplasmic) solution contained 140 mM K-gluconate, 4 mM NaCl, 1 mM EGTA, 2 mM MgCl$_2$, 0.39 mM CaCl$_2$, 20 mM HEPES (pH was adjusted with KOH to 7.2; free [Ca^{2+}] was 100 nM). The pipette (luminal) solution was a standard extracellular solution (modified Tyrode's: 145 mM NaCl, 5 mM KCl, 2 mM CaCl$_2$, 1 mM MgCl$_2$, 10 mM HEPES, 10 mM glucose; the pH was adjusted with HCl or NaOH to 4.6 or 7.4). Data were collected using an Axopatch 2A patch-clamp amplifier, Digidata 1440, and pClamp 10.2 software (Axon Instruments). Whole-lysosome currents, elicited by voltage ramps from −140 mV to +140 mV and repeated at 4-s intervals, were digitized at 10 kHz and filtered at 2 kHz. All experiments were conducted at room temperature (21−23 °C), and all recordings were analyzed with pClamp 10.2 and Origin 8.0 (OriginLab).

Data Analysis—Data are presented as mean ± S.E. Statistical comparisons were made using analysis of variance (ANOVA) and Student's *t* test. *p* values of < 0.05 were considered statistically significant. *: $p < 0.05$; **: $p < 0.01$.

RESULTS

Lysosomal Localization of P2X4—To study the subcellular localization of P2X4, COS1 cells were immunolabeled with an antibody against the C terminus of P2X4 (Fig. 1*A*). Intracellular P2X4 immunofluorescence was seen in all COS1 cells and at least 50% of the cells displayed clear P2X4-positive intracellular puncta that colocalized with Lamp1, demonstrating a lysosomal localization of endogenous P2X4. To examine if heterologously expressed P2X4 also trafficked to lysosomes, COS1 cells transiently expressing a C-terminal GFP-tagged rat P2X4 (rP2X4-GFP) construct were stained with either the anti-Lamp1 antibody or LysoTracker. Confocal fluorescence imaging revealed that the expressed exogenous P2X4 was also present in organelles positively labeled by Lamp1 and LysoTracker (Fig. 1*B*), confirming the lysosomal localization of the exogenous rP2X4-GFP. To further establish the lysosomal localization of P2X4, untransfected and rP2X4-GFP transfected COS1 cells were homogenized and subjected to two-step density-gradient centrifugations to isolate lysosomal fractions (Fig. 1*C*). The presence of P2X4 in each fraction was compared with that of Lamp1 by Western blotting. As shown in Fig. 1, *D* and *E*, both endogenous and exogenous P2X4 were highly enriched in the lysosomal fractions. Similar results were obtained using HEK293T cells (data not shown).

Lysosomal Localization of ATP—Recently, ATP has been shown to be present in lysosomes of astrocytes (11) and microglia (12). Since P2X4 is expressed in the lysosomes of COS1 cells and HEK293T cells, it is plausible that ATP, the endogenous P2X4 agonist, is also present in lysosomes of these cells. To visualize lysosomal ATP deposition, COS1 cells were co-stained with LysoTracker and quinacrine, a fluorescence dye commonly used to locate intracellular ATP stores (11, 12). As shown in Fig. 2*A*, quinacrine colocalized quite well with LysoTracker. In addition, quinacrine also colocalized well with Texas Red-dextran, another lysosome marker (Fig. 2, *lower panels*). These results
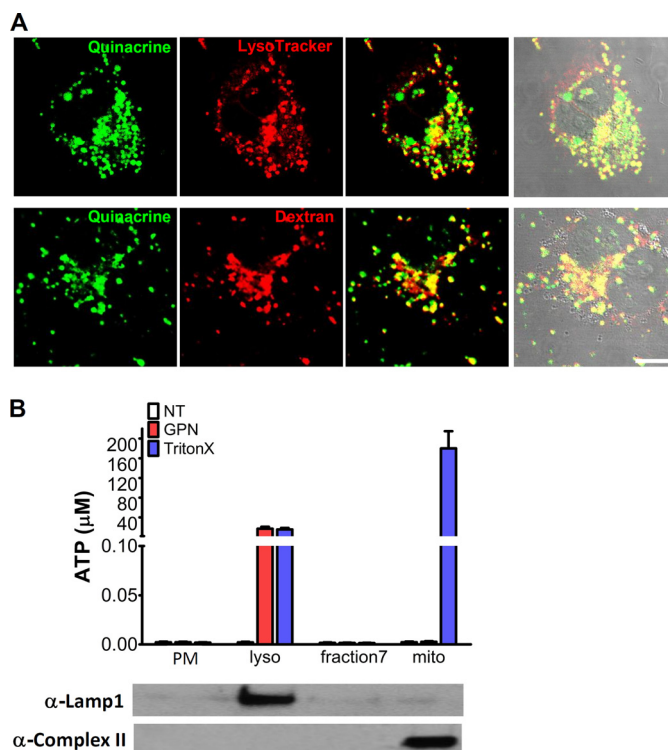

FIGURE 2. Enrichment of ATP in lysosomes. *A*, enrichment of ATP in lysosomes in COS1 cells. ATP was labeled with quinacrine, and lysosomes were stained with either LysoTracker (*upper panels*) or Texas Red 10 kDa dextran (*lower panels*). Scale bars, 10 μm. *B*, ATP contents in subcellular fractions of COS1 cells. Four lysosomal fractions (fractions 2–5) from the two-step density gradient centrifugation as shown in Fig. 1*C* were combined for lysosomal ATP measurement. PM, plasma membrane fraction; *lyso*, lysosomal fractions, *fraction 7*, the fraction collected between lysosomal and mitochondrial fractions; *mito*, mitochondrial fractions (*fractions 8–12* in Fig. 1*C*). Western blots were obtained using 15 μg proteins from each fraction as indicated. Lamp1 was used as a lysosome marker; complex II was used as a mitochondria marker. GPN (200 μM) was used to specifically dialyze lysosomes and Triton X-100 (0.1%) was used to permeabilize all membranes before ATP measurement.

demonstrated the accumulation of ATP in lysosomes of COS1 cells. To further confirm the presence of ATP in lysosomes, ATP contents in the subcellular fractions of COS1 cells isolated by the density gradient centrifugations (as in Fig. 1*C*) were measured using an ATP bioluminescent assay (11, 12). As expected, high concentrations of ATP were only detected in lysosomal and mitochondrial (complex II, a mitochondrial marker) fractions after 5 min of treatment with 1% Triton X-100, indicating the presence of ATP in these membrane-enclosed compartments (Fig. 2*B*). Similar results were also obtained from HEK293T cells (data not shown). Importantly, GPN (200 μM for 30 min), a substrate of the lysosomal exopeptidase cathepsin C that selectively induces lysosome osmolysis (11), selectively released ATP from the lysosomal fractions (Fig. 2*B*), but not mitochondria, validating lysosomes being the source of ATP in these fractions. Taken together, our data indicate that ATP is accumulated in lysosomes of COS1 cells and HEK293T cells, as is the case in astrocytes and microglial cells.

Recording of ATP- and pH-sensitive P2X4 Currents from Lysosomes—The presence of P2X4 in lysosomes could suggest a lysosome function for this channel (2, 13). To directly assess the functionality of lysosomal P2X4, whole-lysosome patch clamp recordings were performed using COS1 cells
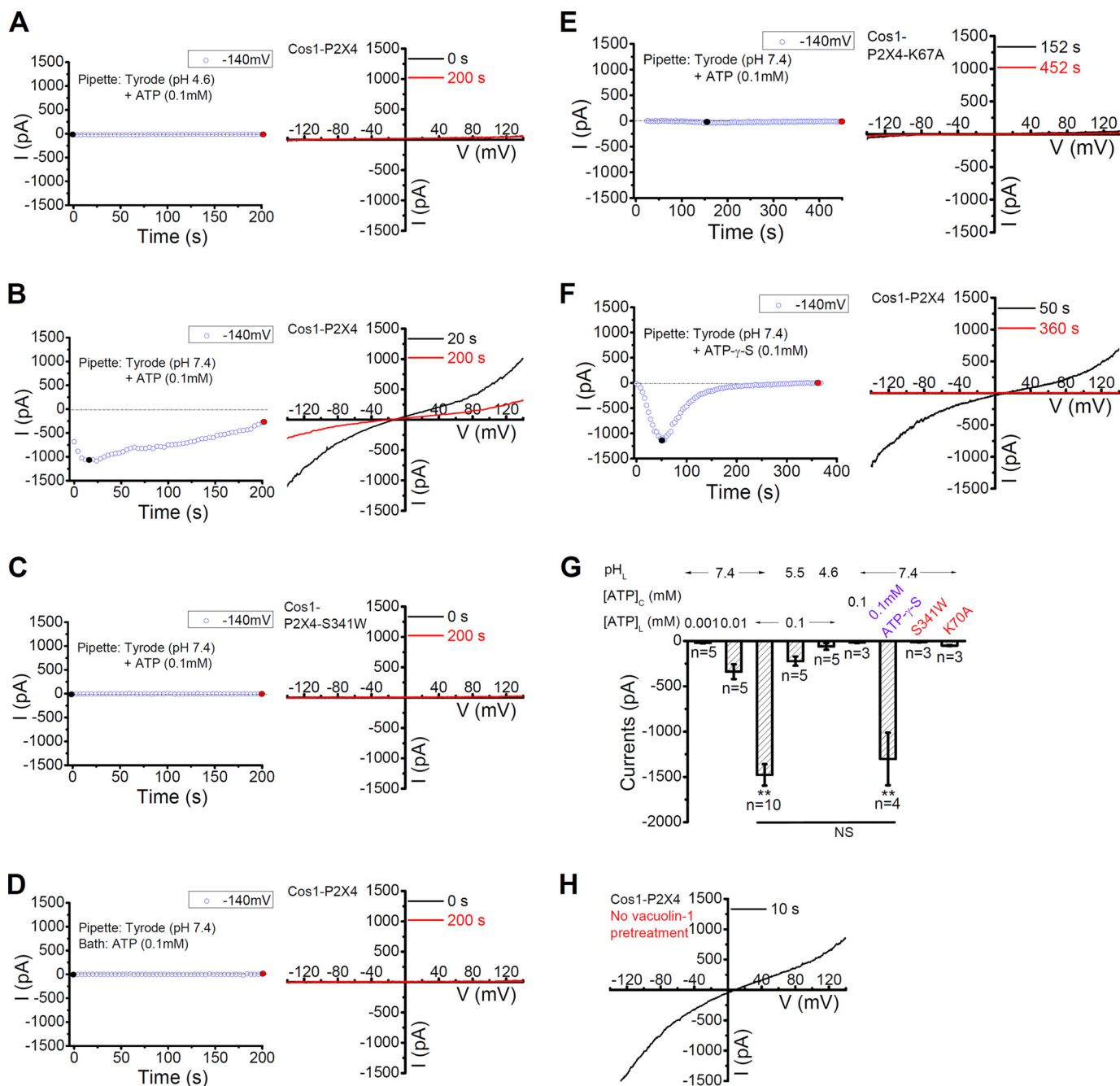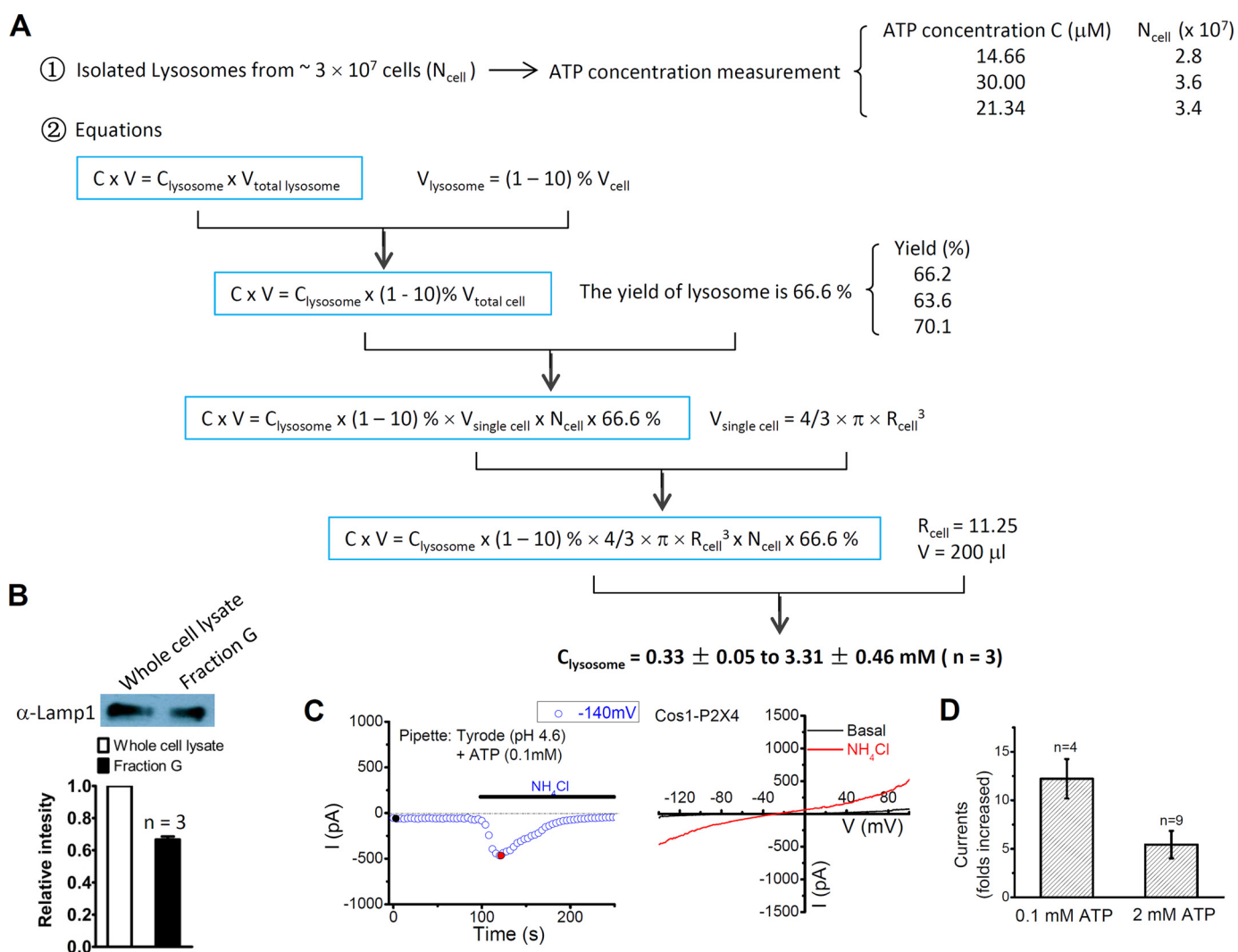
FIGURE 3. **Activation of lysosomal P2X4 by luminal ATP in a dose and pH-dependent manner.** *A*, no current was detected in lysosomes from cells expressing rP2X4-GFP when a pipette solution (lysosome lumen) containing 0.1 mM ATP in pH 4.6 Tyrode was used. For this and subsequent figures, *left*, representative traces of current development at −140 mV; *right*, current-voltage relationships obtained by the voltage ramp at the time points indicated. *B*, large currents were detected with the use of a pipette solution containing 0.1 mM ATP in pH 7.4 Tyrode in lysosomes expressing rP2X4-GFP. *C*, no current was induced by 0.1 mM ATP in pH 7.4 Tyrode in lysosomes expressing rP2X4-S341W-GFP, a non-functional mutant. *D*, application of ATP (0.1 mM) in the bath (cytosolic side) failed to induce current in lysosomes expressing rP2X4-GFP. *E*, little current was induced by pipette infusion of pH 7.4 Tyrode containing 0.1 mM ATP in lysosomes from cells expressing rP2X4-K67A-GFP, an ATP binding deficient mutant. *F*, pipette infusion of 0.1 mM ATP-γS induced large currents in lysosomes expressing rP2X4-GFP. *G*, quantification of currents at −140 mV at conditions as indicated. Lysosomal P2X4 was activated by luminal, but not cytosolic, application of ATP or ATP-γS when the luminal pH was clamped at 7.4. ** ($p < 0.01$) indicates significant difference comparing with the currents induced by luminal 0.1 mM ATP at pH 4.6. *H*, large vacuoles obtained from rP2X4-GFP-transfected COS1 cells without the treatment of vacuolin-1 showed the same current-voltage relationship as the enlarged vacuoles induced by vacuolin-1.

expressing rP2X4-GFP. Most lysosomes were too small for electrophysiological recording using a patch pipette. To overcome this problem, the cells were treated for >2 h with 1 μM vacuolin-1 to promote the formation of enlarged intracellular vacuoles, representing hybrids of late endosomes and lysosomes (9). The vacuoles were released by breaking up the cell

membrane with a sharp glass pipette, and voltage clamping was performed on the vacuole using the conventional whole-cell recording technique, but with the pipette side representing the lysosomal lumen and the bath for cytoplasm. However, with the pipette containing 0.1 mM ATP in the pH 4.6 Tyrode solution (to mimic the acidic pH of lysosomal lumen), little current was

A

① Isolated Lysosomes from ~ 3×10^7 cells (N_{cell}) $\longrightarrow$ ATP concentration measurement

ATP concentration C (µM)	N_{cell} (x 10^7)
14.66	2.8
30.00	3.6
21.34	3.4

② Equations

$$C \times V = C_{lysosome} \times V_{total\ lysosome} \qquad V_{lysosome} = (1-10)\ \%\ V_{cell}$$

$$C \times V = C_{lysosome} \times (1-10)\%\ V_{total\ cell} \qquad \text{The yield of lysosome is 66.6 \%}$$

Yield (%)
66.2
63.6
70.1

$$C \times V = C_{lysosome} \times (1-10)\ \% \times V_{single\ cell} \times N_{cell} \times 66.6\ \% \qquad V_{single\ cell} = 4/3 \times \pi \times R_{cell}^3$$

$$C \times V = C_{lysosome} \times (1-10)\ \% \times 4/3 \times \pi \times R_{cell}^3 \times N_{cell} \times 66.6\ \% \qquad \begin{aligned} R_{cell} &= 11.25 \\ V &= 200\ \mu l \end{aligned}$$

$$C_{lysosome} = 0.33 \pm 0.05 \text{ to } 3.31 \pm 0.46 \text{ mM (n = 3)}$$

B

C

D

FIGURE 4. **Activation of lysosomal P2X4 under physiological conditions.** *A*, schematic diagram showing measurement of ATP concentration in the lysosomal fraction and methods used to estimate ATP concentration in lysosome lumen. *B*, yield of lysosome isolation was determined by measuring the ratio of Lamp1 band intensity in fraction G over that in whole cell lysate. *C*, activation of lysosomal P2X4 by alkalization of intraluminal pH. NH_4Cl induced currents were compared with the basal currents before NH_4Cl application. *D*, summary of currents elicited by NH_4Cl in enlarged lysosomes dialyzed with 0.1 and 2 mM ATP in pH 4.6 Tyrode.

detected from the enlarged lysosomes from cells that expressed rP2X4-GFP (Fig. 3, *A* and *G*). For P2X4 expressed on the PM, it was previously shown that the sensitivity to ATP was strongly attenuated by extracellular acidification but facilitated by extracellular alkalization (14). Therefore, we used the pH 7.4 Tyrode solution in the pipette. Under the whole-lysosome configuration, a large current developed upon pipette dialysis of 0.1 mM ATP in the pH 7.4 Tyrode solution in enlarged vacuoles that expressed rP2X4-GFP (Fig. 3, *B* and *G*). Typically, the current was observed right after the establishment of the whole-lysosome configuration and continued to increase, which was then followed by a gradual decrease presumably because of desensitization (1). The period of current increase was quite variable, likely due to the patch-to-patch differences in dialysis rate. Importantly, the P2X4-like current was not induced in lysosomes from COS1 cells that expressed the non-functional mutant, P2X4-S341W-GFP (Fig. 3, *C* and *G*).

The activation of lysosomal P2X4 by ATP in the pipette suggests that the ATP-binding ectodomain faces lysosomal lumen. To further demonstrate this, ATP was applied to the bath, the cytoplasmic side of lysosomes. As expected, bath application of 0.1 mM ATP did not induce any current in the rP2X4-GFP-expressing lysosomes (Fig. 3, *D* and *G*). For PM P2X4, it was reported that alanine substitution of certain extracellular positively charged amino acid residues in the ATP recognition site(s), such as Lys-67, resulted in a dramatic decrease in ATP potency (15, 16). To further explore the ATP binding site of lysosomal P2X4, lysosomes isolated from cells expressing P2X4-K67A-GFP were recorded, but little current was detected when 0.1 mM ATP was included in the pipettes (Fig. 3, *E* and *G*). Altogether, our data suggest that lysosomal P2X4 is orientated to sense luminal ATP.

The current induced by pipette dialysis of ATP could be caused by products of ATP hydrolysis. To exclude this possibility, a non-hydrolyzable ATP analog, ATP-γS (0.1 mM), was used

and this induced P2X4 currents with similar amplitudes as ATP (Fig. 3, *F* and *G*).

Similar to the P2X4 currents measured on the PM, the lysosomal P2X4 mediated currents displayed both pH- and ATP dose-dependence. The currents evoked by pipette dialysis of ATP (0.1 mM) at pH 5.5 were significantly smaller than that at pH 7.4, but obviously larger than that at pH 4.6 (Fig. 3*G*). At 7.4, 0.01 mM ATP also elicited much smaller currents than 0.1 mM ATP while 1 μM ATP did not evoke any discernible current (Fig. 3*G*).

Since the large lysosomal vacuoles were typically obtained by treating the cells with vacuolin-1, there was a concern that the drug treatment might affect the activation and properties of lysosomal P2X4. To rule out this possibility, naturally occurring large vacuoles obtained from rP2X4-GFP-transfected COS1 cells without the vacuolin-1 treatment were also examined using the whole-lysosome recording technique. These vacuoles also responded to pipette dialysis of 0.1 mM ATP at pH 7.4 with currents that showed similar properties as that seen for the P2X4 channel measured from enlarged vacuoles obtained from vacuolin-1 treated cells (Fig. 3*H*). Therefore, the recorded current properties were unlikely affected by the vacuolin-1 treatment.

Although ATP was shown to be enriched in lysosomes, the concentration of lysosomal ATP was not known. The calculated intravesicular/intragranular ATP concentrations range from 40 μM to 100 mM, depending on the type of vesicles or granules (17–21). Based on ATP content measured from the purified lysosomal fraction (fraction G), the average cell volume, and the proportional volume of lysosomes in a whole cell (1–10%) (8), we estimated the lysosomal ATP concentration ([ATP]$_{lyso}$) to be between 0.33 $\pm$ 0.05 to 3.31 $\pm$ 0.46 mM ($n = 3$) (Fig. 4, *A* and *B*), which falls into the range of calculated ATP concentrations in most vesicles and granules.

To test whether the P2X4 channels on lysosomal membrane are opened under physiological conditions, we recorded enlarged lysosomes using pipettes that contained two different concentrations of ATP, 0.1 mM, which is close to the concentration of pancreatic zymogen granules (17), and 2 mM which is close to other secretory vesicles (18–21). As shown in Fig. 4*C*, although little current was observed after break in when 0.1 mM ATP was included in pH 4.6 Tyrode solution, bath perfusion with 10 mM NH$_4$Cl (pH 7.2), a weak base that increases lysosome pH, induced large currents in lysosomes expressing rP2X4-GFP (from −41.5 $\pm$ 8.8 pA to 458.8 $\pm$ 45.2 pA, $n = 4$). NH$_4$Cl also activated desensitized P2X4 when 2 mM ATP was included in the patch pipette with the pH 4.6 Tyrode solution (Fig. 4*D*). However, NH$_4$Cl itself did not induce any current when no ATP was included in the pipette (data not shown). These data suggest that P2X4 receptors are normally regulated by both ATP and pH in the lysosomes under physiological conditions.

To evaluate whether similar currents could be detected in wild type COS1 cells, enlarged lysosomal vacuoles from vacuolin-1 treated, untransfected, COS1 cells were recorded with pipette dialysis of 1 mM ATP (pH 7.4) under whole-lysosome recording mode. This led to a small P2X4-like current (inward current at −140 mV > 40 pA), which desensitized with time (Fig. 5, *A* and *C*), in lysosomes from 13 out of 27 cells, most
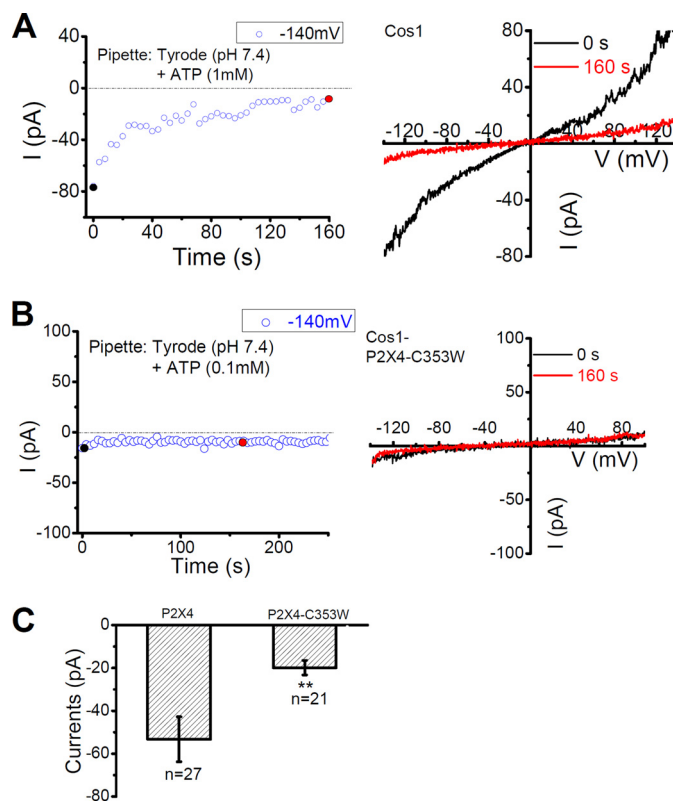
FIGURE 5. **Activation of endogenous P2X4.** *A*, activation of endogenous P2X4-like currents by pipette infusion of 1 mM ATP in pH 7.4 Tyrode in vacuolin-1 enlarged lysosome of an untransfected COS1 cell. *B*, little current was detected in lysosomes expressing P2X4-C353W-GFP, a dominant negative mutant. *C*, mean current amplitudes at −140 mV for P2X4-like currents recorded from enlarged lysosomes of wild type COS1 cells and COS1 cells expressing P2X4-C353W-GFP. **: $p < 0.01$.

likely representing the endogenous lysosomal P2X4 currents. To further determine whether the endogenous P2X4-like current in COS1 cells was mediated by P2X4, we expressed P2X4-C353W-GFP, a dominant negative P2X4 (13, 22, 23) in COS1 cells. Only 3 out of 21 cells showed very small P2X4-like current in enlarged lysosomes (Fig. 5, *B* and *C*).

Pharmacology and Permeation Property of Lysosomal P2X4—The PM P2X4 has been shown to be potentiated by ivermectin (4). To test whether ivermectin also potentiates lysosomal P2X4, 3 μM ivermectin was co-applied with 1 μM ATP, which did not induce P2X4 current (Fig. 6*A*). The inclusion of 3 μM ivermectin with 1 μM ATP in the pipette solution led to the development of a large P2X4 current to a level that was comparable to that induced by dialysis of 0.1 mM ATP (Figs. 6*B* and 5*C*). Average current amplitudes were 1477 $\pm$ 118 pA ($n = 10$) by 0.1 mM ATP (pH 7.4) and 1595 $\pm$ 201 pA ($n = 3$) by 1 μM ATP plus 3 μM ivermectin (pH 7.4).

Like the PM P2X4, lysosomal P2X4 was relatively insensitive to 100 μM suramin (Fig. 6*D*), a generic P2 receptor blocker, and 100 μM PPADS (Fig. 6*E*), a nonspecific P2X receptor antagonist (1). Some P2X receptors, including the PM P2X4, exhibit multiple open states in response to ATP, characterized by a time-dependent increase in the permeability of large organic ions such as *N*-methyl-D-glucamine (NMDG$^+$) (1). Consistent with this property, the lysosomal P2X4 was also permeable to NMDG$^+$, no matter it was applied from the luminal or the

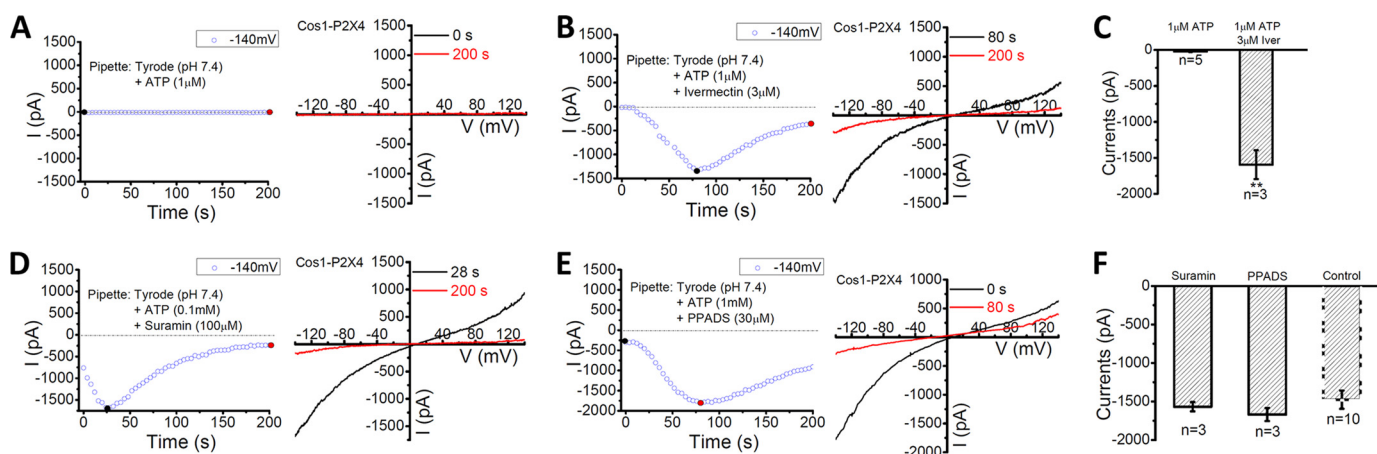FIGURE 6. **Pharmacology of lysosomal P2X4.** *A-C*, although pipette infusion of 1 μM ATP induced little current (*A*), pipette infusion of 1 μM ATP and 3 μM ivermectin induced large currents in lysosomes expressing rP2X4-GFP (*B*). Quantification of currents at -140 mV shows strong potentiation of lysosomal P2X4 activity by 3 μM ivermectin of application of 1 μM ATP at pH 7.4 from the luminal side (*C*). **: $p < 0.01$. *D*, Suramin, a generic P2 receptor blocker, did not block the large currents induced by pipette infusion of 0.1 mM ATP. *E*, PPADS, a nonspecific P2X receptor antagonist, did not inhibit the large currents induced by pipette infusion of 0.1 mM ATP. *F*, quantification of currents at -140 mV at conditions as indicated. Lysosomal P2X4 currents induced by 0.1 mM ATP in the lumen were insensitive to the two common P2 receptor antagonists. Control data are the same as that shown in Fig. 3*G*.
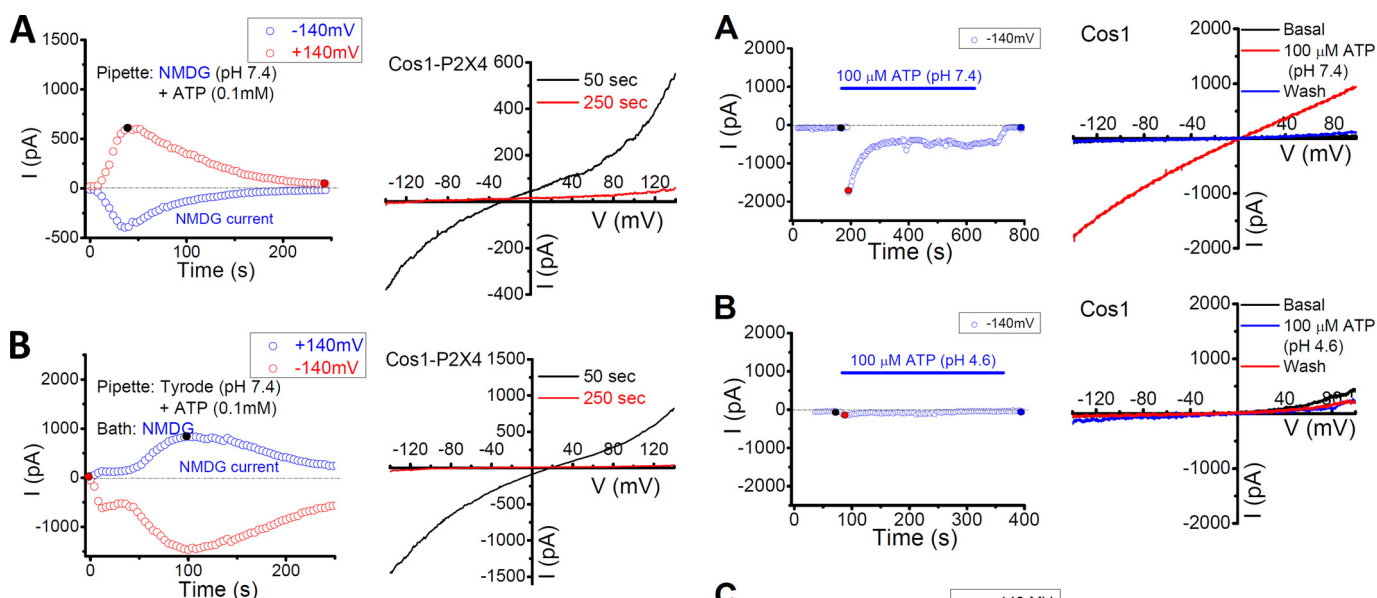

FIGURE 7. **Permeability of lysosomal P2X4 to large cation NMDG$^+$.** *A*, large inward currents (toward cytoplasm) induced by 0.1 mM luminal ATP when the pipette included NMDG$^+$ as the sole cation, suggesting that the activated P2X4 is permeable to luminal NMDG$^+$. *B*, large outward currents (toward the lumen) induced by 0.1 mM luminal ATP when the bath included NMDG$^+$ as the sole cation, suggesting that the activated P2X4 is permeable to cytosolic NMDG$^+$.

cytoplasmic side (Fig. 7). On average, the ratio of inward/outward current amplitudes at the peak was $94.5 \pm 16.3\%$ ($n = 5$) when NMDG$^+$ was applied from the luminal side. Taken together, the P2X4 channels expressed on lysosomes displayed the same pharmacology and permeation properties as their PM counterparts (Fig. 8).

DISCUSSION

In this study, we demonstrated that P2X4 functioned as an ion channel activated by ATP commonly present within the lysosomal lumen, but was kept silent by the acidic pH. The electrophysiological properties and pharmacology of lysosomal P2X4 channels are not different from the same channels
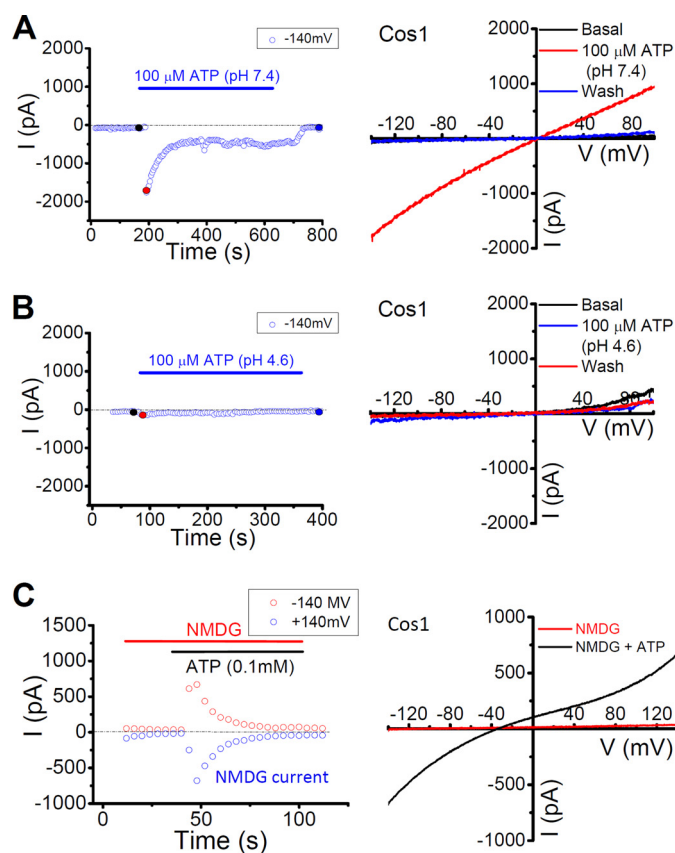

FIGURE 8. **Characterization of P2X4 currents in the plasma membrane.** *A*, large P2X4 currents were induced by bath application of 0.1 mM ATP at neutral pH (pH 7.4) in COS1 cells expressing P2X4-GFP. *B*, little P2X4 current was detected with bath application of 0.1 mM ATP in an acidic (pH 4.6) solution. *C*, plasma membrane P2X4 was NMDG$^+$ permeable. Large inward currents induced by 0.1 mM ATP when the external solution contained NMDG$^+$ as the sole cation.

expressed on the PM. However, our data suggest that the lysosomal P2X4 channels may be constantly exposed to the agonist, ATP. Therefore, the regulation of the lysosomal P2X4 should be different from that of the PM P2X4 channels. Consistent with finding that P2X4 activity in the PM was suppressed by

acidic pH but facilitated by basic pH, we demonstrated that the P2X4 channels expressed in lysosomal membranes were inhibited by the resting lysosomal pH (~pH 4.6) and alkalization of the lysosomal pH relieved such inhibition. This suggests that the lysosomal P2X4 channels are tightly regulated by the luminal pH of the lysosomes, and they are normally inactivated or minimally activated at the resting lysosomal pH (4.5–5.0). The acidic pH in the lysosomal lumen is maintained mainly by the action of vacuolar H^+-ATPases (24) and a cation counterflux (25). It is possible that under certain conditions, *e.g.* the shut down or removal of vacuolar H^+-ATPases, alterations in counter-ion fluxes, or during apoptosis (26), the luminal pH of the lysosome will increase, leading to activation of the lysosomal P2X4. It is also possible that the local pH surrounding the lysosomal P2X4 channels is dynamically regulated in a spatiotemporal fashion, providing a more precise control of the channel function. Therefore, compared with ATP, the luminal pH probably plays a more significant role in regulating P2X4 channel function on the lysosomal membranes and such regulation may be important for lysosome physiology.

The activation of lysosomal P2X4 by luminal (0.1 mM ATP in pipette) but not cytosolic ATP (0.1 mM ATP in bath) would suggest the presence of the ATP-binding/sensing site at the luminal side. This would be consistent with the orientation of the P2X channel found in the intracellular contractile vacuoles of *Dictyostelium discoideum* (27, 28), as well as that of the PM P2X4, in which ATP binds to the extracellular loop (15), with both the N and C termini placed at the cytoplasmic side. Accordingly, the P2X4-K67A mutant, which bears a much reduced sensitivity to ATP (15, 16), was not activated by 0.1 mM ATP from the luminal side. The protective role of *N*-glycans with regards to degradation of receptor also argues for orientation of P2X4 in lysosomes having the expected extracellular domain at the luminal side (2).

Our study suggests that P2X4 receptors are not only present on the lysosomal membranes but also function as cation channels in a luminal pH-dependent manner. Previously, intracellular P2X4 was suggested to mediate physiological functions after being recycled back to the PM (2). Recently, the intracellular P2X channels were found to play important roles in vesicle fusion with the PM in *Dictyostelium discoideum* and in alveolar type II epithelial cells (13, 29). These observations suggest that the lysosomal P2X4 channels are not just a reserve for regulating availability of P2X4 channels on the PM (2). These channels most likely are specifically targeted to the acidic vesicles for unique lysosome-related functions, such as lysosomal trafficking.

Supporting the above argument, lysosomes have been suggested to be another intracellular Ca^{2+} storage site important for many Ca^{2+} signaling processes (30–32). Recently, transient receptor potential mucolipin 1 (6, 9, 33), transient receptor potential melastatin 2 (34, 35), and two-pore channels (36, 37) have been implicated as Ca^{2+} release channels localized on lysosomal membranes. Since the Ca^{2+} permeability of P2X4 has been well established (1, 3), our study expands the research of lysosomal Ca^{2+} signaling by adding another Ca^{2+} permeable channel on the lysosomal membranes. Our findings should

promote further work on elucidating the physiological significance of P2X4 in lysosomal function.

REFERENCES

1. Khakh, B. S., and North, R. A. (2012) Neuromodulation by extracellular ATP and P2X receptors in the CNS. *Neuron* **76,** 51–69
2. Qureshi, O. S., Paramasivam, A., Yu, J. C., and Murrell-Lagnado, R. D. (2007) Regulation of P2X4 receptors by lysosomal targeting, glycan protection and exocytosis. *J. Cell Science* **120,** 3838–3849
3. North, R. A. (2002) Molecular physiology of P2X receptors. *Physiol. Rev.* **82,** 1013–1067
4. Priel, A., and Silberberg, S. D. (2004) Mechanism of ivermectin facilitation of human P2X4 receptor channels. *J. Gen. Physiol.* **123,** 281–293
5. Royle, S. J., Bobanovi, L. K., and Murrell-Lagnado, R. D. (2002) Identification of a non-canonical tyrosine-based endocytic motif in an ionotropic receptor. *J. Biol. Chem.* **277,** 35378–35385
6. Dong, X. P., Shen, D., Wang, X., Dawson, T., Li, X., Zhang, Q., Cheng, X., Zhang, Y., Weisman, L. S., Delling, M., and Xu, H. (2010) PI(3,5)P(2) controls membrane trafficking by direct activation of mucolipin Ca(2+) release channels in the endolysosome. *Nature Commun.* **1,** 38
7. Graves, A. R., Curran, P. K., Smith, C. L., and Mindell, J. A. (2008) The Cl-/H+ antiporter ClC-7 is the primary chloride permeation pathway in lysosomes. *Nature* **453,** 788–792
8. Holtzman, E. (1989) *Cellular Organelles*, Plenum Press, New York
9. Dong, X. P., Cheng, X., Mills, E., Delling, M., Wang, F., Kurz, T., and Xu, H. (2008) The type IV mucolipidosis-associated protein TRPML1 is an endolysosomal iron release channel. *Nature* **455,** 992–996
10. Huynh, C., and Andrews, N. W. (2005) The small chemical vacuolin-1 alters the morphology of lysosomes without inhibiting Ca^{2+}-regulated exocytosis. *EMBO Rep.* **6,** 843–847
11. Zhang, Z., Chen, G., Zhou, W., Song, A., Xu, T., Luo, Q., Wang, W., Gu, X. S., and Duan, S. (2007) Regulated ATP release from astrocytes through lysosome exocytosis. *Nature Cell Biol.* **9,** 945–953
12. Dou, Y., Wu, H. J., Li, H. Q., Qin, S., Wang, Y. E., Li, J., Lou, H. F., Chen, Z., Li, X. M., Luo, Q. M., and Duan, S. (2012) Microglial migration mediated by ATP-induced ATP release from lysosomes. *Cell Res.* **22,** 1022–1033
13. Miklavc, P., Mair, N., Wittekindt, O. H., Haller, T., Dietl, P., Felder, E., Timmler, M., and Frick, M. (2011) Fusion-activated Ca^{2+} entry via vesicular P2X4 receptors promotes fusion pore opening and exocytotic content release in pneumocytes. *Proc. Natl. Acad. Sci. U. S.A.* **108,** 14503–14508
14. Clarke, C. E., Benham, C. D., Bridges, A., George, A. R., and Meadows, H. J. (2000) Mutation of histidine 286 of the human P2X4 purinoceptor removes extracellular pH sensitivity. *J. Physiol.* **523,** 697–703
15. Hattori, M., and Gouaux, E. (2012) Molecular mechanism of ATP binding and ion channel activation in P2X receptors. *Nature* **485,** 207–212
16. Chataigneau, T., Lemoine, D., and Grutter, T. (2013) Exploring the ATP-binding site of P2X receptors. *Front. Cell. Neurosci.* **7,** 273
17. Haanes, K. A., and Novak, I. (2010) ATP storage and uptake by isolated pancreatic zymogen granules. *Biochem. J.* **429,** 303–311
18. Sawada, K., Echigo, N., Juge, N., Miyaji, T., Otsuka, M., Omote, H., Yamamoto, A., and Moriyama, Y. (2008) Identification of a vesicular nucleotide transporter. *Proc. Natl. Acad. Sci. U. S.A.* **105,** 5683–5686
19. Pankratov, Y., Lalo, U., Verkhratsky, A., and North, R. A. (2006) Vesicular release of ATP at central synapses. *Pflugers Archiv : Eur. J. Physiol.* **452,** 589–597
20. Zalk, R., and Shoshan-Barmatz, V. (2006) Characterization of DIDS-sensitive ATP accumulation in brain synaptic vesicles. *FEBS Lett.* **580,** 5894–5898
21. Burnstock, G. (2007) Physiology and pathophysiology of purinergic neu-

rotransmission. *Physiol. Rev.* **87,** 659–797

22. Silberberg, S. D., Chang, T. H., and Swartz, K. J. (2005) Secondary structure and gating årearrangements of transmembrane segments in rat P2X4 receptor channels. *J. Gen. Physiol.* **125,** 347–359

23. Guo, C., Masin, M., Qureshi, O. S., and Murrell-Lagnado, R. D. (2007) Evidence for functional P2X4/P2X7 heteromeric receptors. *Mol. Pharmacol.* **72,** 1447–1456

24. Mindell, J. A. (2012) Lysosomal acidification mechanisms. *Annu. Rev. Physiol.* **74,** 69–86

25. Steinberg, B. E., Huynh, K. K., Brodovitch, A., Jabs, S., Stauber, T., Jentsch, T. J., and Grinstein, S. (2010) A cation counterflux supports lysosomal acidification. *J. Cell Biol.* **189,** 1171–1186

26. Nilsson, C., Johansson, U., Johansson, A. C., Kågedal, K., and Ollinger, K. (2006) Cytosolic acidification and lysosomal alkalinization during TNF-α induced apoptosis in U937 cells. *Apoptosis* **11,** 1149–1159

27. Sivaramakrishnan, V., and Fountain, S. J. (2012) A mechanism of intracellular P2X receptor activation. *J. Biol. Chem.* **287,** 28315–28326

28. Fountain, S. J., Parkinson, K., Young, M. T., Cao, L., Thompson, C. R., and North, R. A. (2007) An intracellular P2X receptor required for osmoregulation in Dictyostelium discoideum. *Nature* **448,** 200–203

29. Parkinson, K., Baines, A. E., Keller, T., Gruenheit, N., Bragg, L., North, R. A., and Thompson, C. R. (2014) Calcium-dependent regulation of Rab activation and vesicle fusion by an intracellular P2X ion channel. *Nature Cell Biol.* **16,** 87–98

30. Morgan, A. J., Platt, F. M., Lloyd-Evans, E., and Galione, A. (2011) Molecular mechanisms of endolysosomal Ca^{2+} signalling in health and disease. *Biochem. J.* **439,** 349–374

31. Lloyd-Evans, E., and Platt, F. M. (2011) Lysosomal Ca(2+) homeostasis: role in pathogenesis of lysosomal storage diseases. *Cell Calcium* **50,** 200–205

32. Patel, S., and Muallem, S. (2011) Acidic Ca(2+) stores come to the fore. *Cell Calcium* **50,** 109–112

33. Dong, X. P., Wang, X., and Xu, H. (2010) TRP channels of intracellular membranes. *J. Neurochem.* **113,** 313–328

34. Lange, I., Yamamoto, S., Partida-Sanchez, S., Mori, Y., Fleig, A., and Penner, R. (2009) TRPM2 functions as a lysosomal Ca^{2+}-release channel in beta cells. *Science Signaling* **2,** ra23

35. Sumoza-Toledo, A., Lange, I., Cortado, H., Bhagat, H., Mori, Y., Fleig, A., Penner, R., and Partida-Sanchez, S. (2011) Dendritic cell maturation and chemotaxis is regulated by TRPM2-mediated lysosomal Ca2+ release. *FASEB J.* **25,** 3529–3542

36. Calcraft, P. J., Ruas, M., Pan, Z., Cheng, X., Arredouani, A., Hao, X., Tang, J., Rietdorf, K., Teboul, L., Chuang, K. T., Lin, P., Xiao, R., Wang, C., Zhu, Y., Lin, Y., Wyatt, C. N., Parrington, J., Ma, J., Evans, A. M., Galione, A., and Zhu, M. X. (2009) NAADP mobilizes calcium from acidic organelles through two-pore channels. *Nature* **459,** 596–600

37. Brailoiu, E., Churamani, D., Cai, X., Schrlau, M. G., Brailoiu, G. C., Gao, X., Hooper, R., Boulware, M. J., Dun, N. J., Marchant, J. S., and Patel, S. (2009) Essential requirement for two-pore channel 1 in NAADP-mediated calcium signaling. *J. Cell Biol.* **186,** 201–209